J10.6

PRECIPITATION DEVELOPMENT IN CONVECTIVE CLOUDS OVER THE EASTERN ARABIAN PENISULA

Daniel Breed[1*], Tara Jensen[1], Roelof Bruintjes[1], Stuart Piketh[2], Abudulla Al Mangoosh[3], and Abdulla Al Mandoos[3]
[1]National Center for Atmospheric Research, Boulder, Colorado, USA
[2]University of Witswatersrand, Johannesburg, Republic of South Africa
[3]Department of Water Resources Studies, Abu Dhabi, United Arab Emirates

1. BACKGROUND

Over the last four years, a number of airborne field studies have been conducted in the United Arab Emirates (UAE) as part of a feasibility study to assess the potential for rainfall enhancement via cloud seeding. A number of aspects were addressed including trace gas and aerosol characterizations, hygroscopic flare development, radar reflectivity measurements, hydrological studies, cloud seeding trials, numerical model simulations, and collection of cloud microphysical data. Detailed information from the 2001-2002 field projects can be viewed at our project Website: www.rap.ucar.edu/projects/UAE.

During the summer, the studies have concentrated on investigating convective clouds forming over the Al Hajir Mountains, known more generally as the Oman Mountains, along and east of the border between the UAE and Oman in the eastern region of the Arabian Penisula. Climatologically, January through March is the peak rainfall period in the UAE (although most recording stations are well away from the mountains), which is caused by the occasional westerly trough and frontal system passing through the region and providing extended periods of rainfall. However, summertime convection contributes a significant (and less variable) portion of the total annual precipitation in the eastern Arabian Peninsula.

The characteristics of summer convective storms resemble those of air mass storms in other sub-tropical regions. The majority are relatively short-lived although long-lived multi-cellular systems exist that produce a large fraction of the total precipitation from summer storms. Figure 1 shows a plot of the duration of storms from the summers of 2001 and 2002 as defined by a 30 dBZ threshold (via the TITAN software). The data are from the Al Dhafra radar, which: 1) was not consistently calibrated through the data collection period; 2) was west of the convection over the mountains by 120 km or more; and 3) was only completing a volume scan every 10 min. Because of the relatively poor temporal and spatial resolution of the data, the TITAN analysis may have limitations. Nonetheless, more detailed data taken in 2003 and 2004 show similar trends in storm duration. The 30-dBZ echo tops of the 2001-2002 storms (not shown) averaged about 8.5 km MSL with 10% of the tops greater than 11 km.

*Corresponding author address: Daniel Breed, NCAR/RAP, P.O. Box 3000, Boulder, CO 80307-3000
email: breed@ucar.edu

During the summers of 2003 and 2004, a randomized seeding experiment was conducted using hygroscopic flares ignited in updrafts at cloud base. A major component of this experiment included making airborne microphysical measurements designed to elucidate the development of precipitation in order to verify steps in the conceptual seeding model. Some of those steps involve drizzle formation and recirculation or dispersion throughout the treated cell or turret and into neighboring turrets. The role of drizzle and larger drops in the graupel formation and riming processes is also viewed as integral to precipitation development (and enhancement) in these storms.

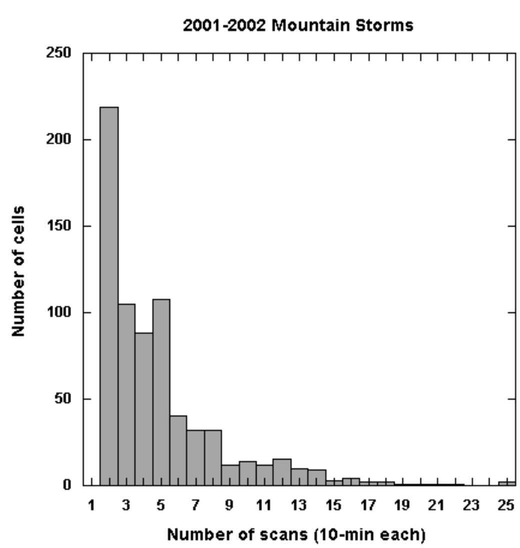

Figure 1. Histogram of cell duration (in number of volume scans) for 715 storms over the Oman mountains in 2001 and 2002. One volume is 10 min (i.e., 6 equals 1 hr).

While conceptually straightforward, the microphysical details of individual cases are not usually as clear and multiple cases are needed to generalize the results. Several cases from the summers of 2003 and 2004 are being synthesized to examine the validity of the conceptual model, and one of them from 12 September 2004 is described in some detail here. The radar data are from a C-band radar, located at Al Ain airport about 40-80 km from the storms described below. Volume scans of 11 elevation angles were completed every 5 min, and the data were reduced in realtime onto a 750 m grid. (The data are currently being reprocessed onto a 500 m grid for better resolution during analysis.) Microphysical data were collected using the South African Aerocommander aircraft with a suite of PMS probes as well as the usual sensors measuring state parameters.

2. 12 SEPT 2004 - Initial Storm Characteristics

The 12Z sounding from Abu Dhabi (Figure 2), taken about 120 km west of the area of interest, shows characteristics of the thermodynamic structure in which summer storms develop. Most prominent is the dry, stable layer beginning near 550 hPa (approximately 5 km and -2° C). The strength of this layer (or lack thereof), caused by large scale subsidence, often determines the formation of storms and their strength. Low-level moisture and mesoscale circulations over the mountains, not represented in the Abu Dhabi sounding, are other major determinants. On the 12th, the stable layer is not particularly strong, suggesting that convection has the potential of pushing through the 400 hPa level to perhaps as high as the 250 hPa level. However, the dryness above 550 hPa also suggests that weaker convective pulses will have suppressed tops.

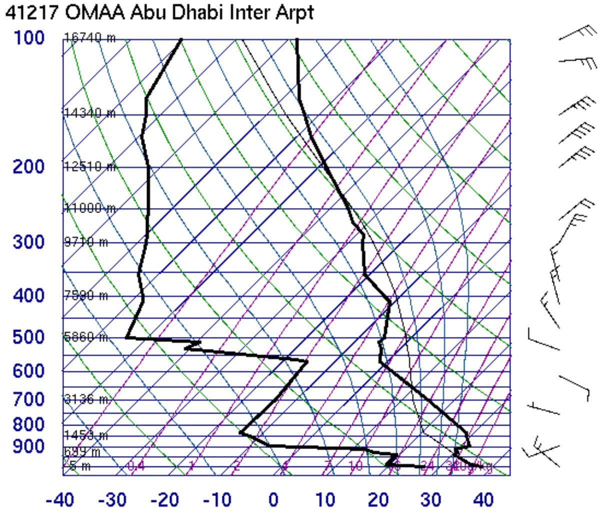

Figure 2. Abu Dhabi sounding (skewT-logP) at 12Z on 12 September 2004. Cloud base was at ~650 hPa. From: http://weather.uwyo.edu/upperair/sounding.html

The first major storm in the operations area developed as part of a second cycle of storms about 70-80 km southeast of Al Ain. The height of the first echoes in the area (~0 dBZ at 10:45) was at 4.5-5.0 km, near the 0° C level. The time-height diagram of maximum reflectivity in Figure 3 shows the multi-cellular nature of the major storm, which formed in a particularly favored region over the mountains for convective development. The appearance of reflectivity (>20 dBZ) at multiple levels suggests the rapid development of precipitation, which is not surprising given the pre-conditioning and potential particle recycling from earlier cells.

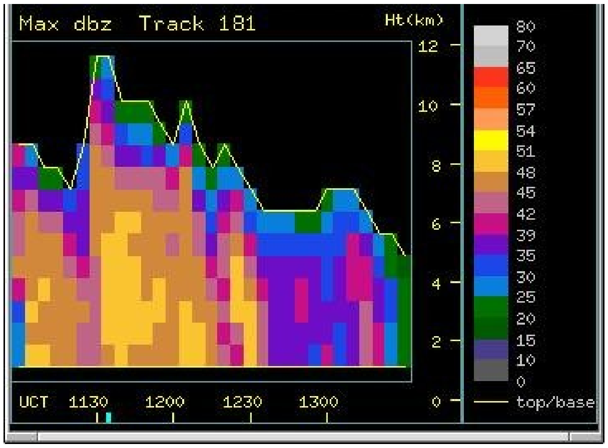

Figure 3. Time-height diagram of maximum reflectivity (>20 dBZ) for the initial storm on 12 Sept 2004. Maximum tops reached about 11 km at 11:35. Note that the color scale is not in equal steps above 35 dBZ.

At 11:35, the storm consists of two main cells (Figure 4). The top reaches ~11 km although the large majority of the mass is below 6.5 km. A cross-section from northwest to southeast through the core of the cells is shown in Figure 5. The hint of a detrainment layer is evident at 4–6 km, particularly on the southeast (downwind) side of the northwest cell.

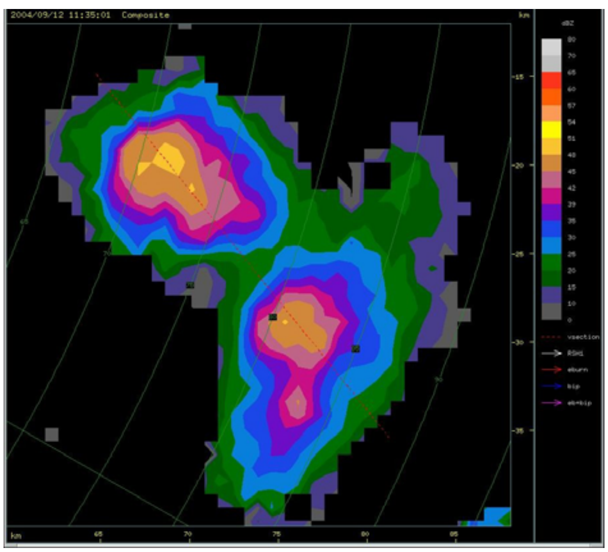

Figure 4. CAPPI of composite reflectivity (maximum dBZ at any level) at 11:35 on 12 Sept 2004. Area is about 27 km x 27 km; green range rings are shown every 5 km; and the dashed red line (from the northwest to the southeast) shows the location of the cross-section in Figure 5.

The photograph in Figure 6 was taken as the research aircraft approached the area at 12:10. Although the time-height diagram indicates that the storm is still active, the photo generally shows the storm tops to be dissipating. The thin iced cloud to the right of center is the remains of the southeast cell of Figure 4, while the top of the northwest cell (center of photo) is beginning to detach. A new but small cell is growing to the left of the larger cell. Also evident is the extensive cloudy region and detrainment layer at roughly the aircraft altitude of 5 km.

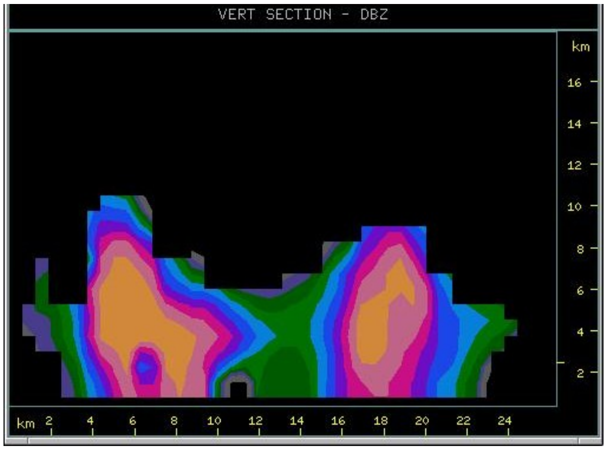

Figure 5. Cross-section of the cells in Figure 4, northwest (left) to southeast (right), at 11:35.

Figure 6. Photo of the initial storm system taken from the research aircraft at 12:10 and 5 km altitude. The dark swath across the lower left of the photo reflects glass changes in the windscreen; and the stray dark spots are debris on the windscreen.

3. 12 SEPT 2004 – Case Study Storm

3.1 Radar

After sampling cells near the major storm, such as the left-most turret in the Figure 6 photo, and cells farther north, the research aircraft settled on a growing cloud mass about 50 km east of Al Ain at 12:50. The time-height diagram of Figure 7 shows the development and decay of the storm, which lasted about 1 hr and looks uni-cellular. In fact, about three different updraft pulses and two moderate reflectivity cores occurred over this time period, reflecting the small-scale complexity of precipitation development under close examination. The top of this storm is considerably lower than the initial storm, and the bulk of the mass is below 6 km. Maximum reflectivities are several dB less as well.

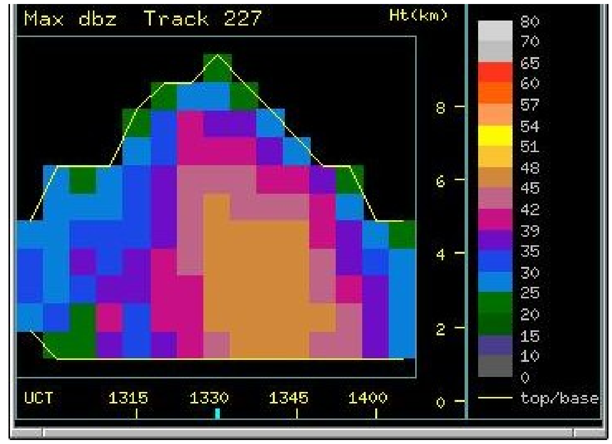

Figure 7. Time-height diagram of maximum reflectivity (>20 dBZ) for the case study storm on 12 Sept 2004. Maximum tops reached about 9 km at 13:30. Note that the color scale is not in equal steps above 35 dBZ.

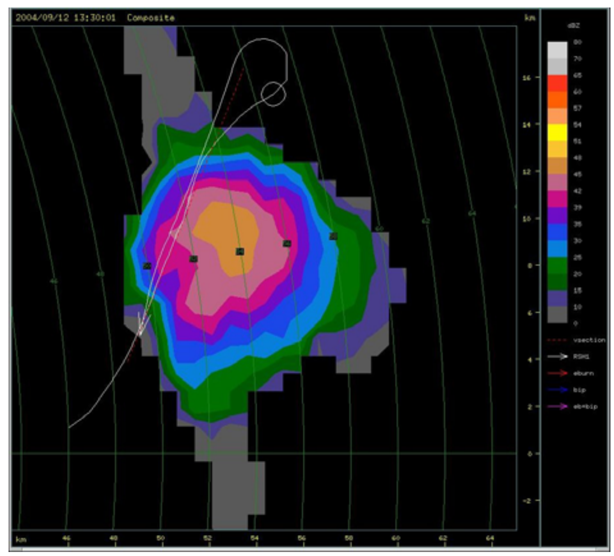

Figure 8. CAPPI of composite reflectivity (maximum dBZ at any level) at 13:30 on 12 Sept 2004. Area is about 21 km x 21 km; green range rings are shown every 2 km; white line shows the aircraft track from 13:27 to 13:33 (circle is at 13:30); and the dashed red line (north to south) shows the location of the cross-section in Figure 9, along the path of the aircraft track.

The CAPPI in Figure 8 is at the time of the maximum top, although the cross-section plot in Figure 9 is taken along the aircraft track rather than through the storm's core. Side-lobe contamination is evident at roughly 52-54 km range, but the tightest reflectivity gradients can still be seen along the west to north side of the cell. More particles appear to be spreading out in the southeast quadrant, which is the downwind side, at a height of around 6 km or less. The cross-section in Figure 9 verifies the detrainment layer at 5-6 km, particularly on the south end of the aircraft track. The echo top at 13:30 along the aircraft track is less than 8 km even though the penetration was visually guided through the most active part of the cell. A cross-section through the core at 13:35 (not shown) verifies that the maximum top was around 9 km with a substantial region of detrained reflectivity at 5-6 km – greatest on the south side.

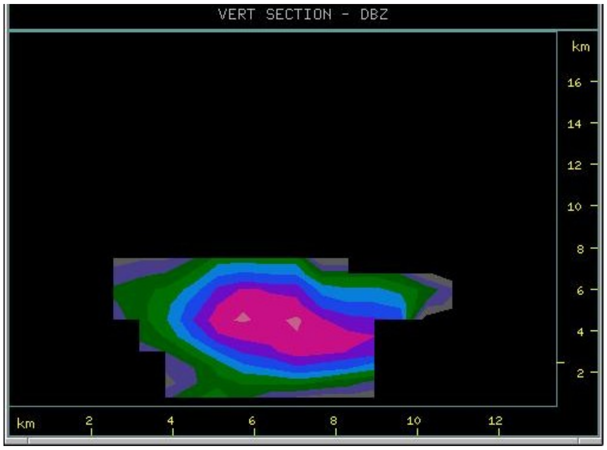

Figure 9. Cross-section of the case study cell in Figure 8, north (left) to south (right) along the aircraft track, at 13:30.

3.2 Aircraft

Seventeen cloud penetrations were made over the course of about 70 min (12:51-13:59), the last four being in the precipitation shaft below cloud base. A short 5-min break from penetrations occurred after 13:00 to deal with wing icing from the first four cloud passes. At 13:01, the cloud base seeding aircraft began 'treatment', which turned out to be a no-seed case for this storm. The best updraft area at cloud base, at least during treatment from 13:01 to 13:16, was in the northwestern quadrant of the cell. The photograph in Figure 10 was taken from the research aircraft, positioned less than 1 km from the cloud mass on the north side and looking south at 13:05. The tops appear to be growing but haven't penetrated much above 7 km. The cloud base aircraft is below the cloud top in the foreground of the photo, just right of center, which is also the target of the cloud penetration.

The photograph in Figure 11 was taken at 13:23:30 at about the same altitude but 3-3.5 km away from the storm on the north side, looking SSW. Over a period of about 20 min, the tops have grown substantially higher and the cloud mass appears to be made up of three or more 'cells'. A significant amount of cloud extends outward at around 6 km (500-1000 m higher than the aircraft).

Time-series plots from the cloud penetration passes shown in Figure 8 are given in Figure 12. The penetrations were made at 5.0 - 5.5 km, corresponding to -2 to -5° C with ~2° buoyant excursions in the updraft on the north side (around 13:28:45 and 13:32:00). Peak droplet concentrations remained quite constant at 650-750 cm^{-3} over the 10 passes up to this time, although the LWC dropped from peaks slightly greater than 2.0 g m^{-3} to 1.5 g m^{-3} or less. An interesting feature that developed on the north side, as shown in the two passes of Figure 12, is the existence of 2DC particles outside of the LWC region. To the aircraft observer, it appeared as though the particles were falling from thin to non-existent cloud. Similar particles and concentrations were sampled on the south side, but within cloudy air (referred to in the observer's notes as 'debris' cloud).

Figure 10. Photo of the case study storm at 13:05, taken from the research aircraft, which was at about 5 km altitude and <1 km away from the cloud mass on the north side (looking south).

Figure 11. Photo of the case study storm at 13:23:30, taken from the research aircraft, which was at about 5 .2 km altitude and 3-3.5 km away from the cloud mass on the north side (looking SSW).

A sample of images from the 2DC at around 13:29 (Figure 13), just on the edge of the updraft in the first pass of Figures 8 and 12, demonstrates a wide range of particle types and sizes. At these temperatures, and especially in updraft, the size of the larger rimed graupel particles suggest frozen drop embryos along with potential recycling of earlier grown particles. There appear to be some drizzle-like images, along with several artifacts (which render the shadow-or counts unreliable for comparison with other passes). A more detailed editing procedure and particle typing algorithm, applied to all the passes, should better determine the development of drizzle formation and the ice phase.

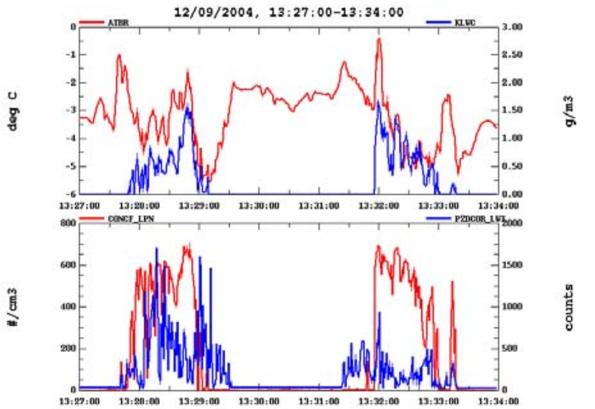

Figure 12. Time series plots on 12 Sept 2004 from 13:27 to13:34 of two penetrations along the same path (as shown in Figure 8). Top plot is temperature (red) with scale on the left and hot-wire liquid water content (blue) with scale on the right. Bottom plot is FSSP concentration (red) with scale on the left and 2DC shadow-or counts (blue) with scale on the right.

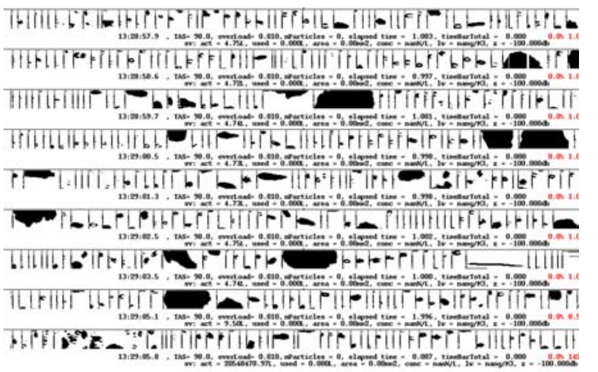

Figure 13. 2DC unedited images (13:28:58 to 13:29:06) on 12 Sept 2004.

4. SUMMARY

The storms that formed on 12 Sept 2004 and described here are fairly typical of storm conditions over the Oman Mountains in the summer. A ubiquitous subsidence inversion often suppresses convection. A weakening of the inversion, coupled with other factors such as low-level moisture or circulations creating convergence zones, leads to cycling of convective clouds and storms and often to the formation of precipitation. The radar data on the 12th show that earlier convection likely pre-conditioned the region with mid-level moisture and ice particles. Subsequent cells and storms developed significant precipitation as they grew above 6 km (around -5° C). This is consistent with the concept that recycling particles into the same and adjacent turrets is an important process in precipitation development. Since no seeding occurred in these storms, the question remains whether a seeding technique designed to increase drizzle formation would have helped the precipitation process in the ‘second shift storms, or helped to increase particles in the initial storms, or had no effect since the process might have already been efficient. More details from the other penetrations on this day and from cases on other days (both seeded and unseeded) should shed light on these possibilities. Certainly, the UAE studies re-emphasize the potential that polarimetric radar information could have in delineating the precipitation process over a wide range of conditions.

5. ACKNOWLEDGEMENTS

This research was funded by the Department of Water Resources Studies of the President’s Office in the United Arab Emirates. Thanks are due to all the field project participants, too numerous to mention, whose skill and hard work made the collection of these data so successful.